JOURNAL OF SOLID STATE CHEMISTRY **122,** 160–165 (1996)
ARTICLE NO. 0097

Lattice Instability in $Li(Li_xMn_{2-x})O_4$

Atsuo Yamada

Sony Corporation Research Center, 174, Fujitsuka-cho, Hodogaya-ku, Yokohama-shi, 240 Japan

Received August 16, 1995; accepted November 22, 1995

The lattice instability in the discharged state of lithium-rich spinel manganese compounds, $Li(Li_xMn_{2-x})O_4$, was investigated with respect to the Jahn–Teller structural phase transition (*Fd*3*m* to $I4_1/amd$) around $T_t = 280$ K in $LiMn_2O_4$. A small amount of excess Li ($0 < x < 0.035$) substituted for Mn (16*d* sites) increased the average Mn valency, suppressing the Jahn–Teller effect and hence stabilizing the cubic phase to drastically decrease both the transition temperature T_t from 282 to 214 K and the latent heat ΔH from 226 to 29 cal/mol. No transition was observed in the region $x > 0.035$, which corresponds to merely <2% Li substitution for Mn. The lattice instability in the charged state was also investigated by comparing the theoretical and the experimental capacity of $Li(Li_xMn_{2-x})O_4$. The cell capacity showed a clear deviation from the theoretical value in the small x region ($x < 0.15$), indicating the mechanical lattice instability induced by scarcity of Li^+ (8*a*). The value of Li substitution x which will maximize the cell performance is discussed.

INTRODUCTION

Layered $LiCoO_2$, $LiNiO_2$(*R*3*m*) (1), and spinel $LiMn_2O_4$(*Fd*3*m*) (2, 3) are materials which can be applied to cathodes of rechargeable lithium ion batteries because of their high voltage (about 4 V) and good rechargeability. Among these materials, $LiMn_2O_4$ is favored over other materials in terms of the manufacturing cost and respect for the environment, being cheap and nontoxic. However, it has a problem in commercial applications; i.e., its rechargeable capacity and cyclability in the 4-V region are inferior to that of layered materials and Mn corrosion occurs in an electrolyte.

Several attempts to improve the poor capacity and cyclability in the 4-V region of $LiMn_2O_4$ have been reported. Low-valent cation doping to 16*d* sites, $Li(M_xMn_{2-x})O_4$ $M^{y+}: y < 3.5$, is a candidate because it reduces the Mn^{3+} content and stabilizes the cubic structure in the face of Mn^{3+} Jahn–Teller distortion (4). Monovalent Li doping seems to be best for several reasons. First, Li^+ provides a larger valence difference relative to Mn than divalent or trivalent cations; hence a small amount of dopant is effective. This minimizes the system randomness which may localize the charge carriers, Li^+ and e^-. Second, migration of non-Li ions to tetrahedral 8*a* sites, which lowers the rechargeable capacity in the 4-V region, can be prevented. That is, the migration or the exchange of doped Li^+ between 16*d* and 8*a* sites, which would be prior to the migration of Mn, results in no decrease in rechargeable capacity.

Gummow *et al*. recently synthesized Li-rich spinel $Li(Li_xMn_{2-x})O_4$ by reacting $LiOH \cdot H_2O$ and γ-MnO_2 (CMD), and reported that cyclic stability in the 4-V region is significantly enhanced at the expense of rechargeable capacity (5). They also discussed the improved cyclic performance of $Li(Li_xMn_{2-x})O_4$ in terms of lattice stability in the vicinity of $y = 3.5$ in Mn^{y+}, the onset of the Jahn–Teller effect, in a deeply discharged state. However, nobody has ever found quantitative evidence to directly indicate that the cubic (*Fd*3*m*) phase is stabilized in the face of Jahn–Teller distortion when a small amount of manganese in the spinel cathode is replaced with lithium or another element which increases the Mn valency.

In this paper, we have investigated the synthesis of a Li-rich spinel, $Li(Li_xMn_{2-x})O_4$, by reacting $LiMn_2O_4$ and Li_2CO_3 with a range of temperature and oxygen pressure, the results of which are presented. We also report that the Jahn–Teller structural phase transition from *Fd*3*m* to $I4_1/amd$ around 280 K in $LiMn_2O_4$ (6) is quite sensitive and so is a good parameter to cation nonstoichiometry x. This sensitivity directly demonstrates that the charge-compensating electrons occupy the Mn 3*d* band, affecting the *Fd*3*m*-phase stability in the face of a Jahn–Teller distortion. The change in the transition temperature T_t and in latent heat ΔH was investigated in detail as a function of Li substitution x, using differential scanning calorimetric (DSC) analysis. The electrochemical capacity in the 4-V region of a coin-type cell containing a $Li(Li_xMn_{2-x})O_4$ cathode was also investigated. The capacity deviation from the theoretical value in the small x region was discussed in terms of the lattice instability induced by the scarcity of Li^+ (8*a*) in the fully charged state. Finally, the value of x which will maximize the cell performance is discussed.

0022-4596/96 $18.00

EXPERIMENTAL

$LiMn_2O_4$ powder was prepared by reacting Li_2CO_3 and Mn_2O_3. The starting materials, Li_2CO_3 (99.99%) and Mn_2O_3 (99.9%) powders, were coarsely mixed at a 1:2 Li:Mn ratio and ball milled for about 24 h in ethanol. After evaporating the ethanol at 70°C, the samples were reground and calcined at 750°C in air. Subsequently they were fired at 850°C in O_2 for 24 h and slowly cooled to room temperature (<5°C/min).

Next, $LiMn_2O_4$ and Li_2CO_3 were mixed in various molar ratios and calcined to obtain Li-rich spinels. The firing temperature and the oxygen pressure were changed to adjust the oxidation power. Generally, the oxidation power has a maximum around 400°C at a constant oxygen partial pressure. In a constant temperature, a higher oxygen partial pressure provides a higher oxidation power. Synthesis in high-pressure oxygen of 200 atm (1,050 atm of 19% O_2/81% Ar mixed gas) was also performed with a hot isostatic pressure (HIP) apparatus (O_2-Dr.HIP, Kobe Steel Co.). Powder X-ray data with Cu$K\alpha$ radiation were collected using the $\theta - 2\theta$ mode with a RINT-2000 system (Rigaku Co.).

Differential scanning calorimetric (DSC) measurements were performed for both the heating and the cooling processes at a rate of 10 K/min in the temperature range between 150 and 400 K. The samples, $Li(Li_xMn_{2-x})O_4$ ($0 < x < 0.04$), and α-Al_2O_3 with 99.999% purity as a standard were weighed to 50 mg and were packed into small aluminum cells to be set in the measuring apparatus (Shinku-Rico Co., DSC-7000). The measurements were performed in dry nitrogen of 500 mmHg.

The electrochemical properties of $Li(Li_xMn_{2-x})O_4$ ($0 < x < 0.33$) as cathode materials were evaluated using coin-type cells (size 2025) containing a lithium metal anode. The cathode was a mixture of 80 wt% $Li(Li_xMn_{2-x})O_4$, 15 wt% graphite, and 5 wt% polyvinylidene fluoride (PVdF) binder. The electrolyte was a 1 *M* $LiPF_6$–propylene carbonate/dimethyl carbonate (PC/DMC) solution. The coin cells were fabricated in a dry atmosphere. The cells were cycled between 3.0 and 4.5 V at a current density of 0.25 mA/cm^2 at 23°C.

RESULTS AND DISCUSSION

Powder X-ray diffraction patterns for samples synthesized from $LiMn_2O_4$ and Li_2CO_3 in the molar ratio of 2:1 (Li 100% excess) are shown in Figs. 1 and 2. In Fig. 1, the oxygen pressure was changed at a constant firing temperature of 850°C, whereas in Fig. 2, the firing temperature was varied at a constant oxygen pressure of 1 atm. Treatment in an atmosphere with a higher oxidation power (in a higher oxygen pressure and a lower temperature) suppresses the peak intensity corresponding to γ-Li_2MnO_3 ($C2/c$) and enhances the cubic spinel peaks ($Fd3m$), with a peak shift to higher diffraction angles.

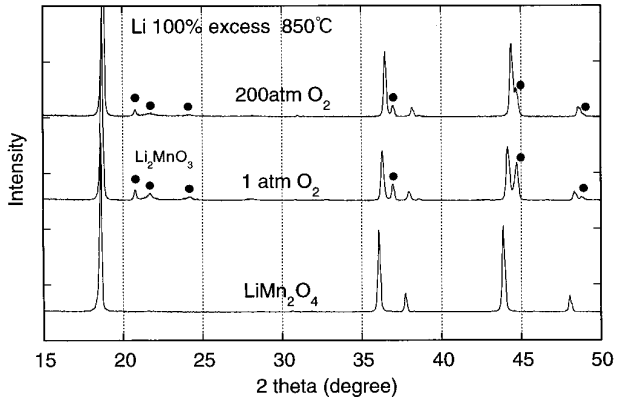

FIG. 1. Powder X-ray diffraction patterns for reaction products of $LiMn_2O_4$ and Li_2CO_3 in the 2:1 molar ratio calcined at 850°C at various oxygen pressures.

This indicates that the excess Li is used to form Li-rich spinel $Li(Li_xMn_{2-x})O_4$ rather than to form γ-Li_2MnO_3 when calcined in an atmosphere with a high oxidation power. Since Mn^{4+} is stabilized relative to Mn^{3+}, i.e., the mean valence of Mn tends to increase ($Mn^{y+}: y > 3.5$) under an oxidation, Li^+ is preferably substituted to Mn 16*d* sites to satisfy the charge neutrality rule and stabilize the cubic structure. In contrast, excess Li^+ would be preferably inserted into the interstitial 16*c* sites (7) under a reducing condition, forming tetragonal $Li_{1+x}Mn_2O_4$ ($Mn^{y+}: y < 3.5$) as can be seen in Fig. 3. Gummow *et al.* recently reported that tetragonal lithiated spinel $Li_2Mn_2O_4$ can be synthesized under appropriate reducing conditions (8).

Consequently, there are two types of Li-rich spinel, $Li[8a](Li_xMn_{2-x})[16d]O_4[32e]$ and $Li[8a]Li_x[16c]Mn_2[16d]O_4[32e]$. The site preference of excess Li depends on

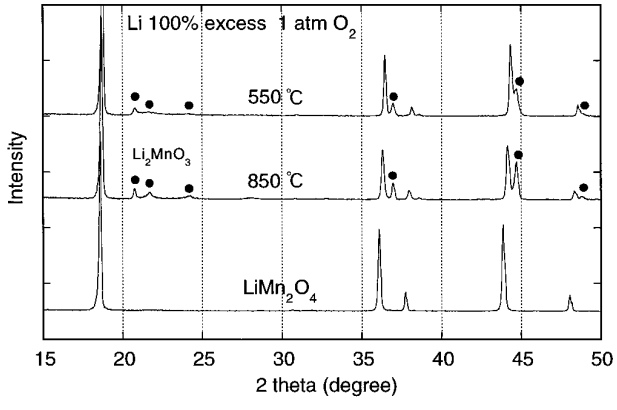

FIG. 2. Powder X-ray diffraction patterns for reaction products of $LiMn_2O_4$ and Li_2CO_3 in the 2:1 molar ratio calcined at various temperatures in 1 atm of oxygen.

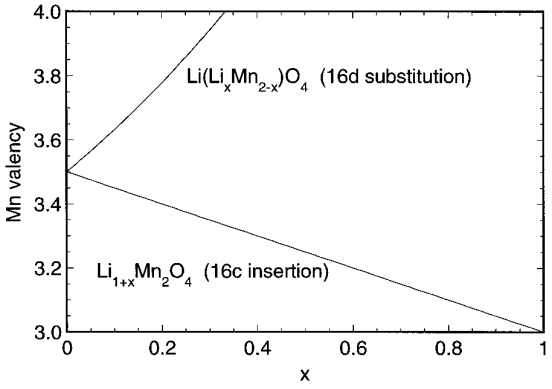

FIG. 3. The relationship between the site preference of excess Li and the Mn valence state.

whether $Mn^{y+}: y > 3.5$ is obtained in oxidation or $Mn^{y+}: y < 3.5$ is obtained in reduction. From a structural aspect, 16*d* substitution in oxidation stabilizes the cubic phase, whereas 16*c* insertion in reduction distabilizes the cubic phase to induce Jahn–Teller distortion with a two-phase ($LiMn_2O_4$ and $Li_2Mn_2O_4$) reaction (9). This is consistent with the fact that the critical mean valence of Mn which induces the cooperative Jahn–Teller effect is 3.5 in Mn spinel oxides and $LiMn_2O_4$ ($Mn^{y+}: y = 3.5$) is just on the critical point (8–11).

Next, the amount of excess Li was varied and calcined in 1 atm of oxygen to confirm the solid solubility limit x_1 in $Li(Li_xMn_{2-x})O_4$. Typical X-ray data are shown in Fig. 4. The peak shift to a higher diffraction angle reaches its maximum, and at the same time, the peaks indexed as γ-Li_2MnO_3 appear when a large amount of Li_2CO_3 is added.

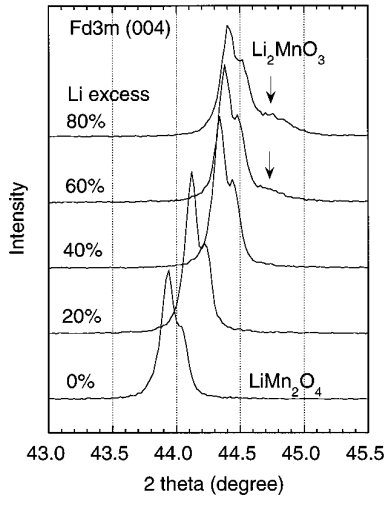

FIG. 4. The change in the powder X-ray diffraction profile of *Fd3m* (004) peak when the amount of excess Li is changed from 0 to 80%. The firing condition is 550°C in O_2 for 15 h.

This means that Li can no longer be incorporated into the spinel phase. The value of x_1, which was estimated from saturated lattice constants, increased from 0.12 to 0.33 as the firing temperature decreased from 850 to 400°C, because of the higher oxidation power at the lower temperatures. At $x = 0.33$, the composition can be denoted as $Li(Li_{1/3}Mn_{5/3})O_4$ or $Li_4Mn_5O_{12}$ in which all Mn are tetravalent, and this is the maximum value of x (see Fig. 3).

DSC curves for $Li(Li_xMn_{2-x})O_4$ ($0 < x < 0.04$) in the temperature range between 150 and 350 K are shown in Fig. 5. The samples used for DSC experiments were synthesized at 650°C in O_2 for 15 h. The reversible exothermic and endothermic peaks with a temperature hysteresis of about 10 K correspond to the first-order structural phase transition from *Fd3m* ($T > T_t$) to $I4_1/amd$ ($T < T_t$) caused by the Jahn–Teller effect of Mn^{3+} (6). Note that only a few percent of Li substitution for Mn have a significant effect on transition behavior. In another words, the transition is very sensitive to cation nonstoichiometry x. The phase transition temperature, T_t, drastically decreases from 282.3 to 214.3 K (DSC peak position in the heating process) when a very small amount of Mn is replaced by Li ($x < 0.033$). At the same time, the latent heat ΔH is suppressed from 226.0 to 28.9 cal/mol (heating process), as plotted in Fig. 6. Finally, the transition disappears at around $x = 0.035$, which corresponds to a mere <2% Li substitution for Mn.

The lattice instability of the cubic phase in the discharged state of spinel Mn oxides can be attributed to the tetragonal distortion caused by the cooperative Jahn–Teller effect of Mn^{3+} in octahedral sites, and hence is affected by the following two factors: the valence state of Mn and the temperature.

(i) Valence state of Mn (8–11): The tetragonal lattice distortion induced around Mn^{3+} ($t_{2g}^3 \cdot e_g^1$) is suppressed by the long-range interaction with the nondistorted region around Mn^{4+} ($t_{2g}^3 \cdot e_g^0$), which are not Jahn–Teller ions. Therefore, $Li_2Mn_2O_4$ ($Mn^{y+}: y = 3.0$) has the largest distortion ($c/a = 1.158$) in the Li–Mn spinel family. This distortion is gradually suppressed as Mn^{4+} ions are introduced to the matrix, to produce, for example, $Li_5Mn_4O_9$ ($y = 3.25$, $c/a = 1.142$), $Li_7Mn_5O_{12}$ ($y = 3.40$, $c/a = 1.108$), or $LiMn_2O_{3.86}$ ($y = 3.36$, $c/a = 1.107$). In $LiMn_2O_4$ ($Mn^{y+}: y = 3.5$), the lattice assumes a cubic symmetry ($c/a = 1$). The cubic phase becomes more stabilized as the average Mn valence approaches 4.0. The tetragonal distortion is also suppressed by a non-Jahn–Teller ion Mn^{2+} ($t_{2g}^3 \cdot e_g^2$), as shown in Fig. 7.

(ii) Temperature change (6): In the high-temperature region ($T > T_t$), the local distortion of the oxygen octahedron in three directions occurs independently. The entropy term (phonon) dominates the cooperative interaction and the direction of the distortion can be dynamically exchanged. Therefore, the average lattice symmetry is cubic.

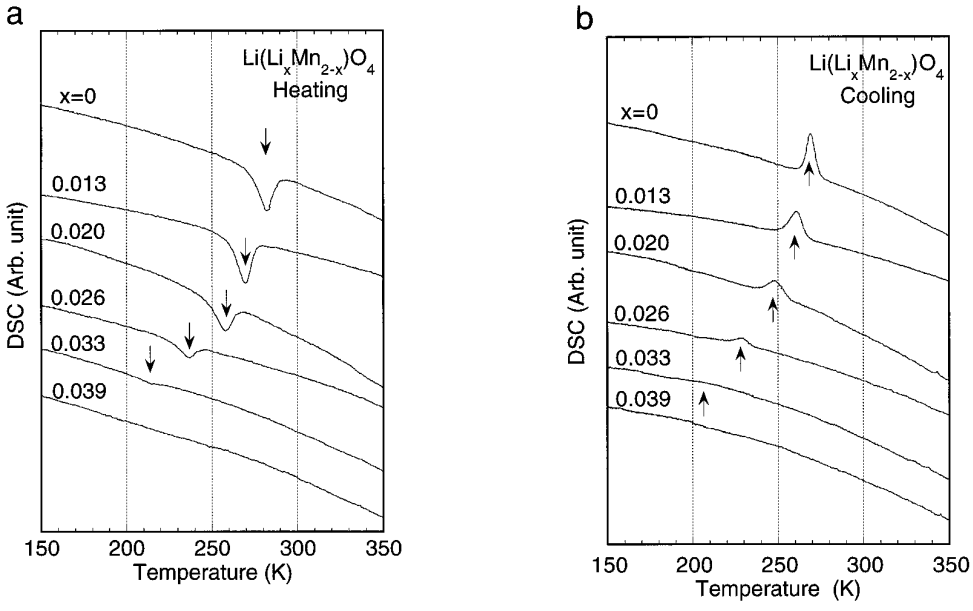

FIG. 5. DSC curves of $Li(Li_xMn_{2-x})O_4$ ($0 < x < 0.04$) measured in the temperature range between 150 and 350 K for (a) heating and (b) cooling processes.

In the low-temperature region, cooperative interaction to minimize the strain energy becomes more important than the entropy effect, and forms a tetragonal ordering state in which all of the distortion occurs in the same direction. However, the low-temperature phase of $LiMn_2O_4$ ($T < T_t = 280$ K) is more complicated: it is characterized by very little lattice distortion ($c/a = 1.011$) and the coexistence of two phases ($I4_1/amd$ and $Fd3m$ in the saturated volume ratio of 65%/35%) (6).

It is clear that factor (i) is much more influential than factor (ii) as the driving force in inducing the Jahn–Teller distortion in $LiMn_2O_4$, as is expected from the small and imperfect phase change in the low temperatures ($T < 280$ K) (6) and from the very steep slope, $d(c/a)/dy$, in the vicinity of $Mn^{y+}: y = 3.5$ in Fig. 7. Therefore, the structural phase transition around 280 K caused by factor (ii) is very sensitive to the amount of Li substitution x which relates to the factor (i) (See Fig. 3). Furthermore, Li substitution is effective in changing the Mn valence state because Li^+ provides a difference of 2 or 3 in the valence number, as compared to the difference of 1 or 2 in the case of substitu-

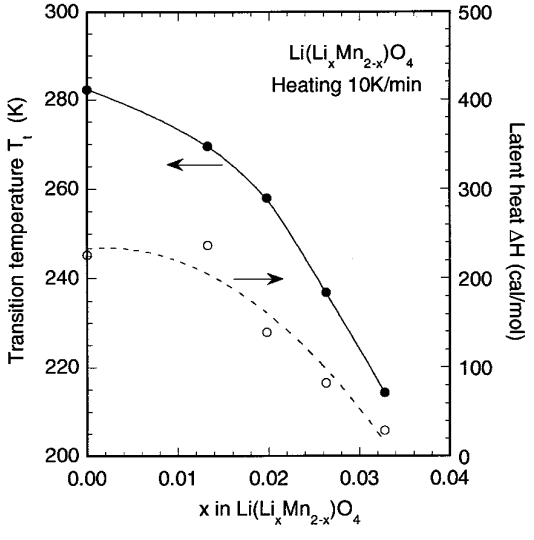

FIG. 6. The change in the phase transition temperature T_t and the latent heat ΔH as a function of Li substitution x in $Li(Li_xMn_{2-x})O_4$.

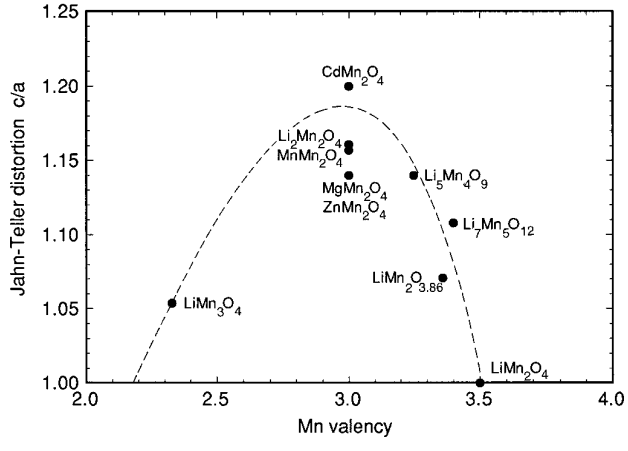

FIG. 7. The suppression of the Jahn–Teller effect of Mn^{3+} by the non-Jahn–Teller ions, Mn^{4+} and Mn^{2+}.

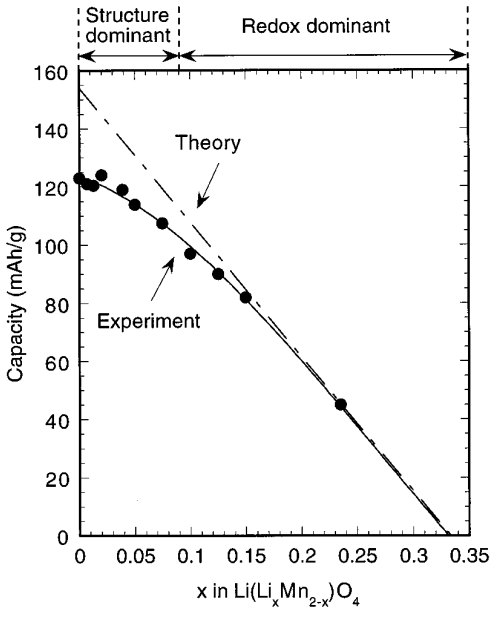

FIG. 8. The first discharge capacity (3.0–4.5 V) of $Li(Li_xMn_{2-x})O_4$ ($0 < x < 0.033$). The broken line is the theoretical capacity based on the Mn^{3+}–Mn^{4+} redox reaction and the mass of the fully oxidized (Mn^{4+}) composition.

tion by another element, such as Mg^{2+}, Zn^{2+}, or a 3*d* transition metal. The large difference in the valence numbers enhances the sensitivity to *x*.

The Jahn–Teller structural phase transition around 280 K in $LiMn_2O_4$ can be used as a measure of the cation nonstoichiometry *x* and hence the Jahn–Teller lattice instability in the discharged state. The lower transition temperature and the smaller latent heat in $Li(Li_xMn_{2-x})O_4$ ($0 < x < 0.04$) directly indicate that charge-compensating electrons occupy the Mn 3*d* band to increase Mn valency and stabilize the cubic phase.

It is not clear whether the 280 K Jahn–Teller transition in $LiMn_2O_4$ affects the low-temperature performance of a cell. If local distortions and lattice dynamics are ignored, the cell performance is not effected by low temperatures because very small and imperfect phase changes in $T < T_t = 280$ K would be cancelled out by the small amount of Li^+ deintercalation with the change in Mn valency during the initial charging (oxidation) process in a cell. However, the performance may be influenced by local distortions which cannot be detected by XRD analysis or by lattice in dynamics in the vicinity of the phase transition such as a soft phonon, which has low elasticity and hence is subject to damped low-frequency, large amplitude vibration. If so, the low-temperature performance of a cell must be improved by a small amount of Li substitution for Mn at a negligible expense to the capacity, as is indicated in Fig. 8. Discussion of this problem is continuing and further investigations are now in progress.

The first discharge capacity is plotted against the Li substitution *x* in Fig. 8. The dotted line is the theoretical capacity based on the Mn^{3+}–Mn^{4+} redox reaction and the mass of the fully oxidized (Mn^{4+}) composition. Theoretical first charge capacity (when Li are extracted) decreases from 154 to 0 mAh/g from $LiMn_2O_4$ to $Li_4Mn_5O_{12}$. In the large *x* region ($x > 0.15$), the spinel lattice remains rigid even in a fully oxidized state because of the many remnant Li ions on 8*a* sites which are electrochemically inactive at 4 V, where the capacity is wholly determined by the Mn^{3+}–Mn^{4+} redox reaction. In the small *x* region ($x < 0.15$), in contrast, there exist few Li ions on 8*a* sites in the fully oxidized state due to the large electrochemical capacity, hence the spinel lattice becomes mechanically unstable before the oxidation to Mn^{4+} is finished in a nonaqueous electrolyte. Therefore, the experimental results deviate from the theoretical values in the small *x* region and show a plateau, in spite of good agreement in the large *x* region. It may be preferable to refer to these composition ranges as ''structure dominant'' (small *x*) and ''redox dominant'' (large *x*) regions, as indicated in Fig. 8.

The amount of capacity deviation from the theoretical value can be used as a measure of the mechanical lattice instability in the charged state caused by the scarcity of Li^+ (8*a*). The larger deviation would present the more destabilized spinel lattice in the charged state, which may relate to the two-phase situation concerning the superlattice ordering of Li ions (9). The detailed mechanism of this deviation, however, cannot specifically be described in this stage of our investigation.

In summary, when $LiMn_2O_4$ is cycled in a cell, there seems to be two kinds of lattice instability, the Jahn–Teller instability in the discharged state and the mechanical instability in the charged state. It is not clear which is dominant to the capacity fading. However, since both of these instabilities can be significantly suppressed by low-valent cation doping to the Mn 16*d* sites with some expense to the rechargeable capacity, the Jahn–Teller structural phase transition around 280 K (the transition temperature T_t and the latent heat ΔH) and the capacity deviation from the theoretical value would be useful parameters in determining the composition of $Li(M_xMn_{2-x})O_4(M^{y+}: y < 3.5)$ which will maximize the cell performance. It is worth noting here that our preliminary investigations on charge-depth dependence of the cyclic performance suggests that the mechanical instability in the charged state is dominant to the capacity fading rather than the Jahn–Teller instability in the discharged state.

In the case of $M = Li$, the composition around the knee point ($x = 0.05$) in Fig. 8, where the lattice instability can be suppressed at a negligible expense to the capacity, as compared with stoichiometric $LiMn_2O_4$, seems to be the best to maximize cell performance. This result is consistent with the previous report by Tarascon *et al.* that the best

powders for battery applications are made by slow cooling of a mixture with the nominal composition $Li_{1.05}Mn_2O_4$ (12), which should really have the composition $Li_{1.05}Mn_2O_{4.067}$ and corresponds to $x = 0.033$ in the notation $Li(Li_xMn_{2-x})O_4$.

CONCLUSION

The Li-rich spinel compounds, $Li(Li_xMn_{2-x})O_4$ ($0 < x < 0.33$), were synthesized from $LiMn_2O_4$ and Li_2CO_3. The solubility limit x_1 was extended by treating under appropriate oxidizing conditions. The Jahn–Teller structural phase transition around 280 K in $LiMn_2O_4$ was quite sensitive to excess Li x, indicating that charge-compensating electrons occupy the Mn 3*d* band and stabilize the cubic phase in the discharged state. The rechargeable capacity of a coin-type cell showed the deviation from the theoretical capacity in the small x region, indicating the mechanical lattice instability in the charging state. Further investigations of the influence of Li substitution on the low-temperature performance of a cell and the optimization of the value of x around 0.05 are still necessary. The phase transition temperature T_t, the latent heat ΔH, and the deviation from theoretical capacity are all useful as parameters to determine the optimum composition.

ACKNOWLEDGMENTS

The author thanks K. Sekai, T. Endo, K. Yamaura, and Y. Iwakoshi for technical discussions, and K. Tanaka for suggestions.

REFERENCES

1. K. Mizushima, P. C. Jones, P. J. Wiseman, and J. B. Goodenough, *Mater. Res. Bull.* **15,** 783 (1980).
2. M. M. Thackeray, W. I. F. David, P. G. Bruce, and J. B. Goodenough, *Mater. Res. Bull.* **18,** 461 (1983).
3. M. M. Thackeray, P. J. Johnson, L. A. de Picciotto, P. G. Bruce, and J. B. Goodenough, *Mater. Res. Bull.* **19,** 179 (1984).
4. J. Yamaki, "Proc. International Workshop on Advanced Batteries, Feb. 22–24, Osaka, Japan." p. 54. 1995.
5. R. J. Gummow, A. de Kock, and M. M. Thackeray, *Solid State Ionics* **69,** 59 (1994).
6. A. Yamada and M. Tanaka, *Mater. Res. Bull.* **30,** 715 (1995).
7. W. I. F. David, M. M. Thackeray, L. A. de Picciotto, and J. B. Goodenough, *J. Solid State Chem.* **67,** 316 (1987).
8. R. J. Gummow and M. M. Thackeray, *J. Electrochem. Soc.* **141,** 1178 (1994).
9. T. Ohzuku, M. Kitagawa, and T. Hirai, *J. Electrochem Soc.* **137,** 769 (1990).
10. A. Yamada, K. Miura, K. Hinokuma, and M. Tanaka, *J. Electrochem. Soc.* **142,** 2149 (1995).
11. K. Miura, A. Yamada, and M. Tanaka, *Electrochimica Acta* **41,** 249 (1996).
12. J. M. Tarascon, F. Coowar, G. Amatuci, F. K. Shokoohi, and D. G. Guyomard, *J. Power Sources* **54,** 103 (1995).